Self-organisation of helically forced MHD flow in confined cylindrical geometries

Malcolm Roberts[1], Kai Schneider, Wouter Bos, Jorge Morales, Matthieu Leroy

Aix-Marseille University

Instabilities and Transport in Magnetized Plasmas, Geophysical and Astrophysical Flows Marseille, 2014-04-15

[1] malcolm.i.w.roberts@gmail.com, www.malcolmiwroberts.com

Simulation of Self-Organization in MHD Flow

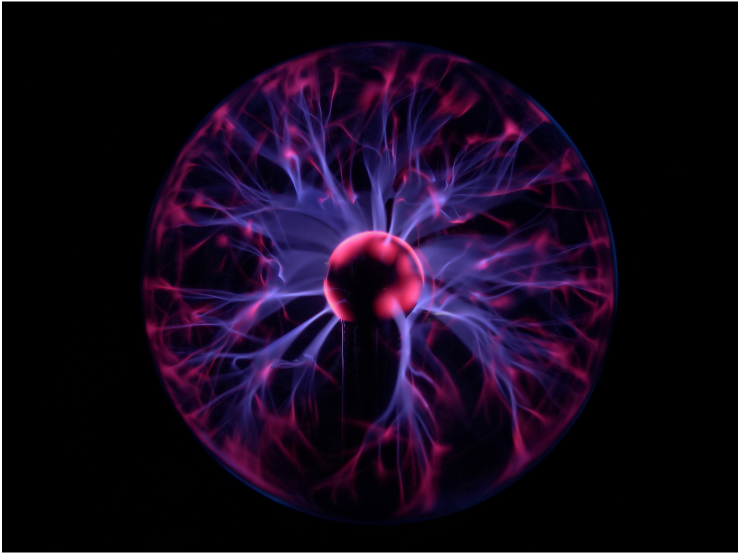

Malcolm Roberts Aix-Marseille University

Outline

- Presentation of model
- Numerical Method
  - Pseudospectral Method
  - Penalty method
  - Method for determining the penalty field
- Simulations with circular cross-section
- Simulations with elliptical cross-section
- Conclusions

Governing Equations: MHD

Let $\boldsymbol{u}$ be the velocity of an electric field with magnetic field $\boldsymbol{B}$.
The velocity changes as

$$\frac{\partial \boldsymbol{u}}{\partial t} = \boldsymbol{u} \times \boldsymbol{\omega} + \boldsymbol{j} \times \boldsymbol{B} - \boldsymbol{\nabla} P + \nu \nabla^2 \boldsymbol{u}$$

where $\boldsymbol{\omega} = \nabla \times \boldsymbol{u}$ is the vorticity, $\boldsymbol{j} = \nabla \times \boldsymbol{B}$ is the current density, P the pressure, and ν is the kinematic viscosity.
The magnetic field changes as

$$\frac{\partial \boldsymbol{B}}{\partial t} = \boldsymbol{\nabla} \times (\boldsymbol{u} \times \boldsymbol{B}) + \lambda \nabla^2 \boldsymbol{B}$$

where λ is the magnetic diffusivity.
We require the velocity and magnetic field be solenoidal:

$$\boldsymbol{\nabla} \cdot \boldsymbol{u} = 0 \qquad \boldsymbol{\nabla} \cdot \boldsymbol{B} = 0$$

Boundary Conditions and Geometry

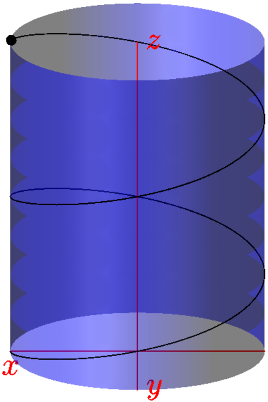

- The fluid is evolved in a periodic cylinder denoted Ω_f.
- The velocity is no-slip:
  - $\boldsymbol{u}|_{\partial\Omega_\mathsf{f}} = \mathbf{0}$
- The magnetic field is forced towards a helix:
  - $B_\perp|_{\partial\Omega_\mathsf{f}} = 0$
  - $B_z|_{\partial\Omega_\mathsf{f}} = B_0$
  - $B_\theta|_{\partial\Omega_\mathsf{f}} = B_c$

The wrapping number of the forcing (the inverse safety factor) is set to integer values.

Boundary Conditions and Geometry

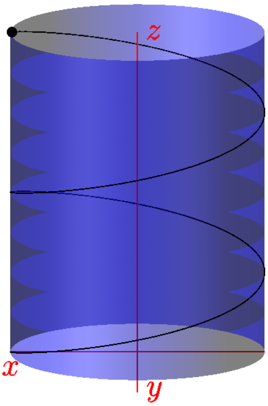

We can also impose an elliptical cross-section, shown here with eccentricity $1/\sqrt{2}$.

Using a level-set approach (for example), very general geometries may be described.

As in the circular case, wrapping numbers are integral.

Initial Conditions and Physical Parameters

Physical parameters:

- $\nu = 4.5 \times 10^{-2}$
- $\lambda = 4.5 \times 10^{-2}$
- Prandtl number is unity.

Geometrical parameters:

- Major radius is set to 1.
- The length of the cylinder in the z-direction is 8.

Initial conditions:

- The magnetic field matches the boundary conditions.
- The velocity field is perturbed with a random field.
- The perturbation has kinetic energy of order 10^{-6}.

Numerical Method

The source terms are computed via the pseudospectral method.

Boundary conditions are imposed via the penalty method.

The system is advanced in time using an Adams-Bashforth method, with Laplacian terms treated implicitly.

Pseudospectral Method

Let $\hat{\boldsymbol{u}}_{\boldsymbol{k}}$ and $\hat{\boldsymbol{B}}_{\boldsymbol{k}}$ be the Fourier transform of $\boldsymbol{u}$ and $\boldsymbol{B}$.
The Fourier transform of the governing equations are

$$\frac{\partial \hat{\boldsymbol{u}}_{\boldsymbol{k}}}{\partial t} = \mathcal{F}\left(\boldsymbol{u} \times \boldsymbol{\omega}\right) + \mathcal{F}\left(\boldsymbol{j} \times \boldsymbol{B}\right) - i\boldsymbol{k}\hat{P}_{\boldsymbol{k}} - \nu k^2 \hat{\boldsymbol{u}}_{\boldsymbol{k}},$$

with the pressure determined via $\nabla \cdot \boldsymbol{u} = 0 \iff i\boldsymbol{k} \cdot \hat{\boldsymbol{u}}_{\boldsymbol{k}} = 0$, and

$$\frac{\partial \hat{\boldsymbol{B}}_{\boldsymbol{k}}}{\partial t} = i\boldsymbol{k} \times \mathcal{F}\left(\boldsymbol{u} \times \boldsymbol{B}\right) - \lambda k^2 \hat{\boldsymbol{B}}_{\boldsymbol{k}}$$

The nonlinear terms are computed by:

- $2/3$-padding the input data
- transforming from Fourier space to physical space
- multiplying the fields
- transforming back into Fourier space.

Pseudospectral Method

The use of FFTs make the pseudospectral method efficient.

FFTs can only be used when the computational domain Ω is a periodic box.

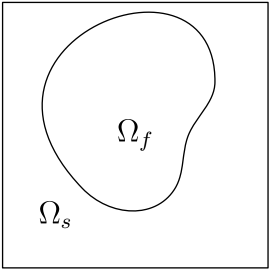

We embed the fluid domain Ω_{f} inside Ω.

The solid domain is $\Omega_{\mathsf{s}} = \Omega/\Omega_{\mathsf{f}}$.

We *penalize* the motion of the fluid in the solid domain with penalization parameter η.

Penalty Method

Let χ_{Ω_s} be the characteristic function for Ω_s.
The penalized velocity evolution equations is

$$\frac{\partial \boldsymbol{u}}{\partial t} = \boldsymbol{u} \times \boldsymbol{\omega} + \boldsymbol{j} \times \boldsymbol{B} - \boldsymbol{\nabla} P + \nu \nabla^2 \boldsymbol{u} - \frac{\chi_{\Omega_s}}{\eta} \boldsymbol{u},$$

corresponding to homogeneous Dirichlet boundary conditions.
The penalized evolution equation for $\boldsymbol{B}$ is

$$\frac{\partial \boldsymbol{B}}{\partial t} = \boldsymbol{\nabla} \times (\boldsymbol{u} \times \boldsymbol{B}) + \lambda \nabla^2 \boldsymbol{B} - \frac{\chi_{\Omega_s}}{\eta} (\boldsymbol{B} - \boldsymbol{B}_s)$$

where $\boldsymbol{B}_s$ is the penalization field.
Source terms are projected onto the solenoidal manifold via a Helmholtz decomposition.

Penalty Method

Advantages:

- Proof of convergence, $\mathcal{O}\left(\sqrt{\eta}\right)$.
- Deals with complex geometries.
- Easy to implement.

Disadvantages:

- Only first-order accurate in space.
- Stiff in time: $dt \approx \eta$.
- Theory mostly developed for Dirichlet boundary conditions.

Current Directions:

- Improving convergence and reducing stiffness.
- Generalizing boundary conditions.

Determining the Penalty Field

The penalty field $\boldsymbol{B}_s$ should

- match the boundary conditions at $\partial\Omega_{\mathsf{f}}$,
- be solenoidal,
- and be as regular as possible.

Determining the Penalty Field

For circular geometries, we can make use of the fact that, in cylindrical coordinates,

$$\hat{\boldsymbol{r}} \cdot \boldsymbol{B}_s = 0,$$

so

$$\boldsymbol{B}_s = B_c f(r)\hat{\boldsymbol{\theta}} + B_0\hat{\boldsymbol{z}}, \tag{1}$$

with $f(r)$ a smooth function that is equal to 1 at the boundary and goes to zero within the periodic box.

The formulation given in equation (1) is necessarily solenoidal.

Similarly, any $\boldsymbol{B}_s$ corresponding to solid-body motion is guaranteed to be both smooth and solenoidal.

Determining the Penalty Field

We can also find such fields in general.

Suppose that we are given boundary conditions $\boldsymbol{v}_{\mathrm{bc}}$ on $\partial\Omega_{\mathsf{f}}$ for the field $\boldsymbol{v}$.

Suppose also that

$$\int_{\partial\Omega_{\mathsf{f}}} \boldsymbol{v}_{\mathrm{bc}} \cdot \hat{\boldsymbol{n}}\, ds = 0,$$

so that the boundary conditions are consistent with a solenoidal field $\boldsymbol{v}$.

We find the penalization field $\boldsymbol{v}_{\mathsf{s}}$ in the computational domain Ω by solving

$$\kappa \nabla^2 \boldsymbol{v}_{\mathsf{s}} - \frac{\chi_{\partial\Omega_{\mathsf{f}}}}{\eta_\tau} \left(\boldsymbol{v}_{\mathsf{s}} - \boldsymbol{v}_{\mathrm{bc}} \right) = 0. \tag{2}$$

Determining the Penalty Field

We solve equation (2) using by pseudo-time-stepping and the pseudospectral method.

The field is made solenoidal by performing a Helmholtz decomposition on $\boldsymbol{v}_{\mathsf{s}}$ after each pseudo-time-step.

Pseudo-time-stepping is stopped when

$$\left\|\boldsymbol{v}_{\mathsf{s}} - \boldsymbol{v}_{\mathrm{bc}}\right\|_{\infty,\partial\Omega_{\mathsf{f}}} < 0.2 \times \sqrt{\eta},$$

which implies that the error in the boundary conditions is less than the expected error from the penalty method.

Simulations: Circular Cross-Section

Simulations were performed on `ada.idris.fr` and `turing.idris.fr`.

- For low forcing amplitudes, the axial velocity was negligible.
- Simulations with $\|(B_0, B_c)\| \gtrapprox 15$ showed exponential growth of the axial kinetic energy.
- The axial kinetic energy eventually reached a stable plateau.
- Increasing wrapping number decreased the axial kinetic energy growth rate.
- The velocity field self-organized into helical pairs.

Simulations: Circular Cross-Section

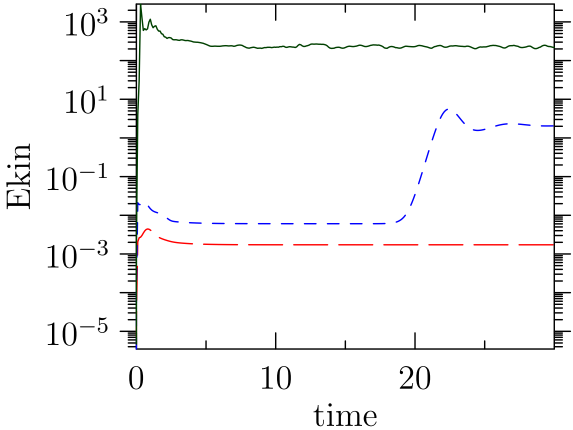

Kinetic energy as a function of time for different forcing parameters.

Simulations: Circular Cross-Section

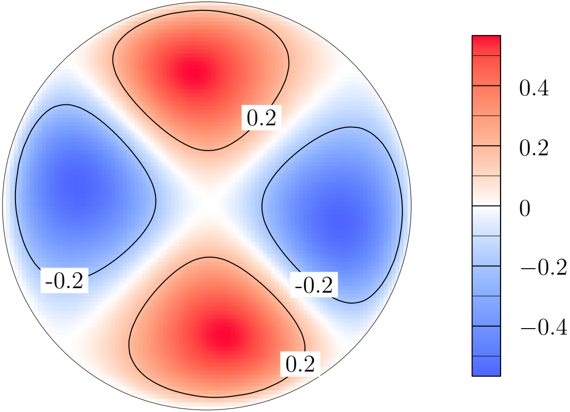

Axial velocity for $B_c = 7.06$, $B_0 = 4.5$, wrapping number 2.

Simulations: Circular Cross-Section

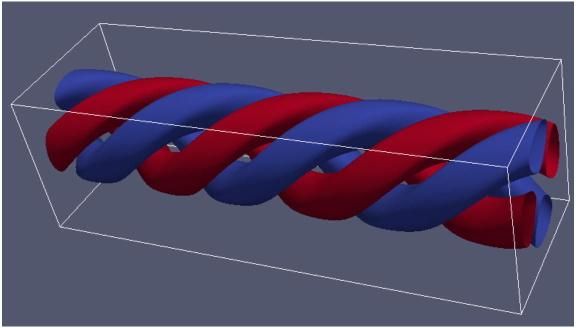

Axial velocity for $B_c = 7.06$, $B_0 = 4.5$, wrapping number 2.

Simulations: Circular Cross-Section

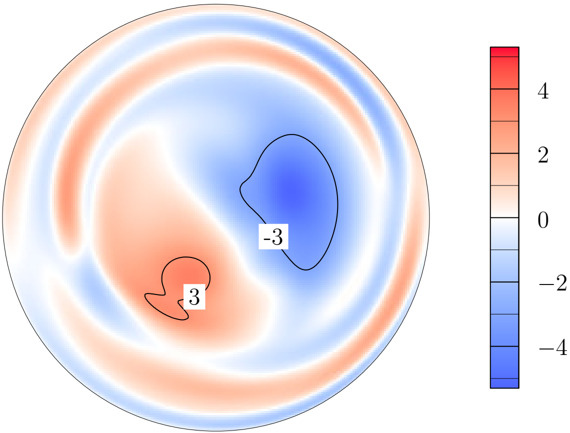

Axial velocity for $B_c = 70.6$, $B_0 = 4.5$, wrapping number 20.

Simulations: Circular Cross-Section

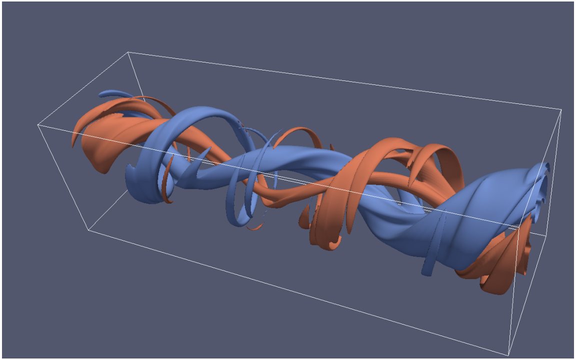

Axial velocity for $B_c = 70.6$, $B_0 = 4.5$, wrapping number 20.

Simulations: Circular Cross-Section

Simulations with circular cross sections exhibited:

- Growth of axial kinetic energy for large forcing amplitude.
- Growth was positively correlated with forcing wrapping number.
- The flow self-organized into a variety of helical modes.
- Large enough energy growth produced a transition to turbulence.
- Turbulent flows were composed of a high-mode boundary layer with a low-order helical mode away from the boundary.

Circular geometries produce helical modes.

By removing symmetries, what happens to the helical modes?

Simulations: Elliptical Cross-Section

Increasing eccentricity suppressed growth of axial kinetic energy.

The first instance of self-organization accrued at $\|(B_0, B_c)\| = 60$ for our simulations.

The mode azimuthal mode-number was much larger than in the circular case.

Simulations: Elliptical Cross-Section

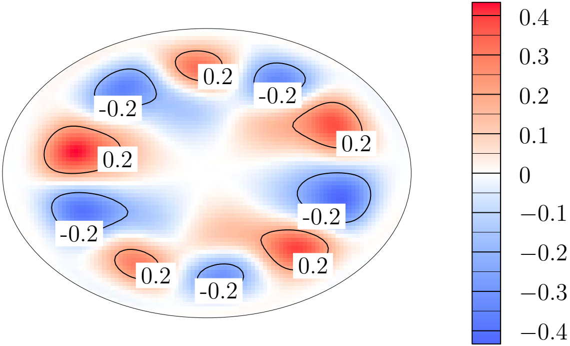

Axial velocity for $B_c = 49.7$, $B_0 = 33.6$, wrapping number 1.

Simulations: Elliptical Cross-Section

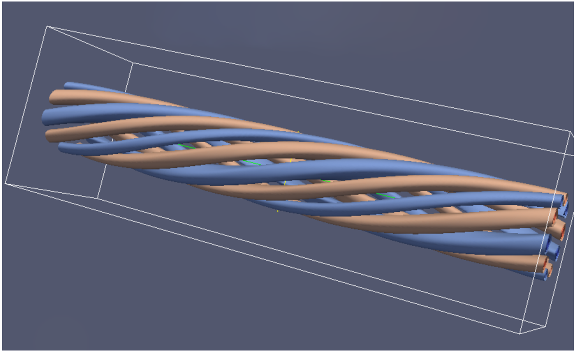

Axial velocity for $B_c = 49.7$, $B_0 = 33.6$, wrapping number 1.

Simulations: Elliptical Cross-Section

The elliptical geometry

- Suppressed axial kinetic energy growth.
- Also exhibited self-organization into helical modes.
- The resulting helical structures had a larger azimuthal modenumber.
- Axial velocity tended to be concentrated farther away from the z-axis than in the circular case.

Alignment of fields

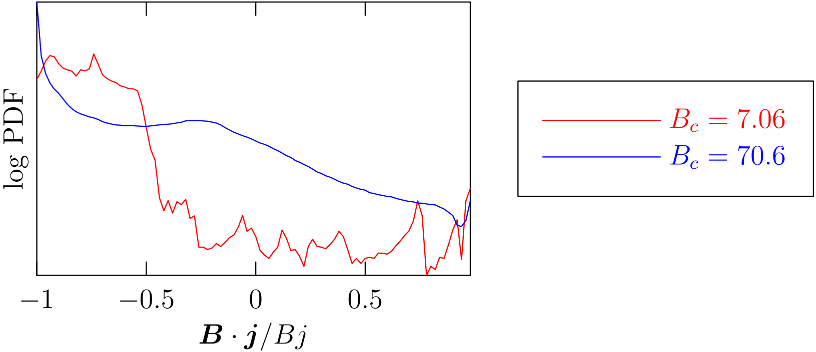

Alignment of $\boldsymbol{B}$ and $\boldsymbol{j}$ (magnetic helicity).

Alignment of fields

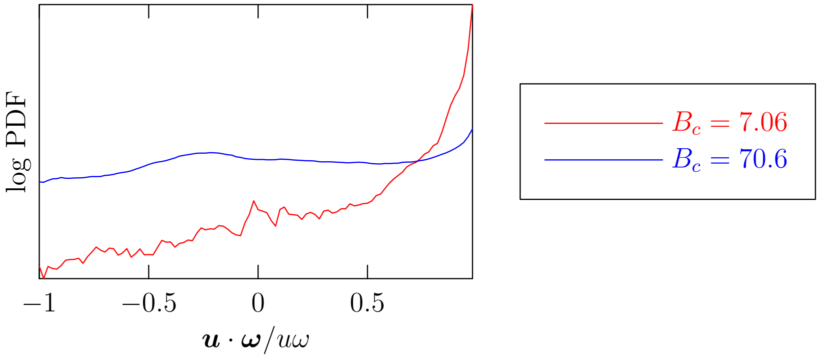

Alignment of $\boldsymbol{u}$ and $\boldsymbol{\omega}$ (kinetic helicity).

Alignment of fields

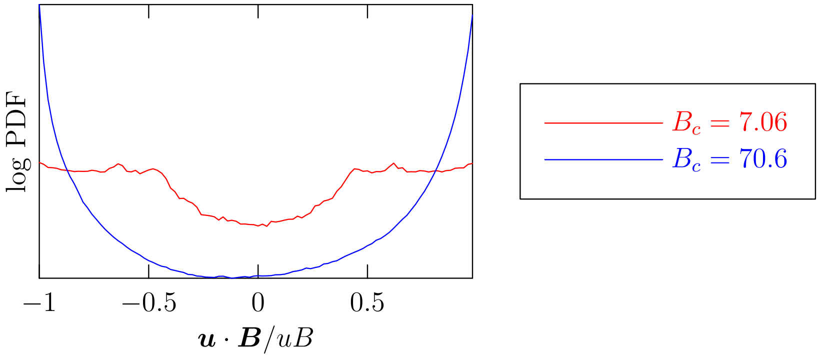

Alignment of $\boldsymbol{u}$ and $\boldsymbol{B}$ (cross helicity).

Summary: Alignment of Fields

- $\boldsymbol{B}$ and $\boldsymbol{j}$ tend to anti-alignment, more so with increasing turbulence.
- $\boldsymbol{u}$ and $\boldsymbol{\omega}$ tend toward alignment, less so with increasing turbulence.
- $\boldsymbol{u}$ and $\boldsymbol{B}$ tend to align or anti-align, very strongly with increasing turbulence.

Conclusions

The goal of this work is the simulation of complex MHD flows. The fluid was confined to a periodic cylinder and the magnetic field helically forced at the boundary.

- The velocity self-organized into helices for sufficiently strong forcing amplitude.
- These helical modes survived even in turbulent regimes.
- Changing the cross-section of the cylinder dramatically changed the flow structure.

Merci pour votre attention!